Catalysis Today 345 (2020) 116–124

Contents lists available at ScienceDirect

Catalysis Today

journal homepage: www.elsevier.com/locate/cattod

The structure-catalytic activity relationship for the transient layered zeolite MCM-56 with MWW topology

Aleksandra Korzeniowska[a], Justyna Grzybek[a], Katarzyna Kałahurska[a], Martin Kubu[b], Wiesław J. Roth[a], Barbara Gil[a,*]

[a] Faculty of Chemistry, Jagiellonian University, Gronostajowa 2, 30-387 Kraków, Poland
[b] Department of Physical and Macromolecular Chemistry, Faculty of Science, Charles University in Prague, Hlavova 8, 128 43 Prague 2, Czech Republic

ARTICLE INFO

Keywords:
Structure-Catalytic activity relationship
MCM-56 zeolite
Friedel-Crafts alkylation
External Brønsted acid sites

ABSTRACT

Zeolite MCM-56 is a high alumina, monolayered form of the commercially useful framework MWW but it is a transient product during crystallization, so many factors influence its state and quality. This work examines properties of a series of MCM-56 and MCM-49 samples synthesized for different times using Aerosil, Ultrasil and Ludox as silica sources, hexamethyleneimine as the structure directing agent and additionally aniline as structure promoting agent. It was found that the most important parameter, governing the catalytic activity in the test reaction of Friedel-Crafts alkylation of mesitylene with benzyl alcohol, was availability of the Brønsted acid centers located at the external surfaces of the crystals. The key role in correlating physical characteristic with activity was played by infrared spectroscopy as it enabled the study of many properties of the tested materials, starting from the total concentration of acid centers, and their type (Brønsted or Lewis acids) through the concentration of centers available for the reagent molecules, to investigating the correlation of acidity with the degree of zeolite crystallinity.

1. Introduction

Zeolites are one of the dominant classes of industrial catalysts used in oil refining and in processes ranging from petrochemistry [1–3] to fine chemical synthesis [4–6], and quite recently have been also intensively studied for various biomedical applications [7–9]. They have framework structures with strictly defined pore sizes, shapes and connectivity that contain variable amounts of active sites. Finding relationships between zeolite channel architecture, acidity and activity in catalytic reactions involving different molecules is one of the most challenging goals in zeolite science even under laboratory conditions. Structure-reactivity relation define how the chemical reactivity of zeolites is related to their chemical structure [10]. In the case of zeolites, this means identification of the real active centers of the reaction, their concentration, environment, i.e. location inside a specific channel or cavity, and also accessibility for the reactant molecules. Such data allows fundamental understanding of the action of a single active site. It is believed that if relationships between material properties and reactivity can be identified, it would allow the design of materials for specific catalytic applications [11,12].

Such in depth understanding at a molecular level can be attempted by applying spectroscopic techniques. In this regard, FTIR spectroscopy offers very useful tools designed for investigation of the properties of catalysts. Quantitative adsorption of probe molecules allows determination of the concentration of the active centers of specific type, i.e. acidic, redox, etc. [13]. For microporous materials, probe molecules can be chosen based on size so that the adsorption is realized only on the external surfaces, or on all centers available in the catalyst [14]. This distinction is useful when materials should be applied as catalysts for reactions with the participation of large reagents, with sizes close to or exceeding channel entrances. Analysis of the FTIR fingerprint region, which is usually applied for determination of the functional fragments of organic molecules of the catalysts, may also provide valuable information of the structure of inorganic materials, such as zeolites. Presence of the specific building units may be directly related to the quality of the material, hence in long term, also performance as a catalyst [15].

For classic 3D zeolites, their channel sizes, usually below 1 nm, may reduce utilization of the active sites located inside micropores due to limited access and slow mass transport [16]. One of many methods to increase the acid site accessibility is specific ‘reduction’ of the size of the crystals, which can be provided by lamellar (2D) zeolites. Such zeolites,

* Corresponding author.
E-mail address: gil@chemia.uj.edu.pl (B. Gil).

https://doi.org/10.1016/j.cattod.2019.09.044
Received 28 June 2019; Received in revised form 22 September 2019; Accepted 25 September 2019
Available online 28 September 2019
0920-5861/ © 2019 The Authors. Published by Elsevier B.V. This is an open access article under the CC BY-NC-ND license (http://creativecommons.org/licenses/BY-NC-ND/4.0/).

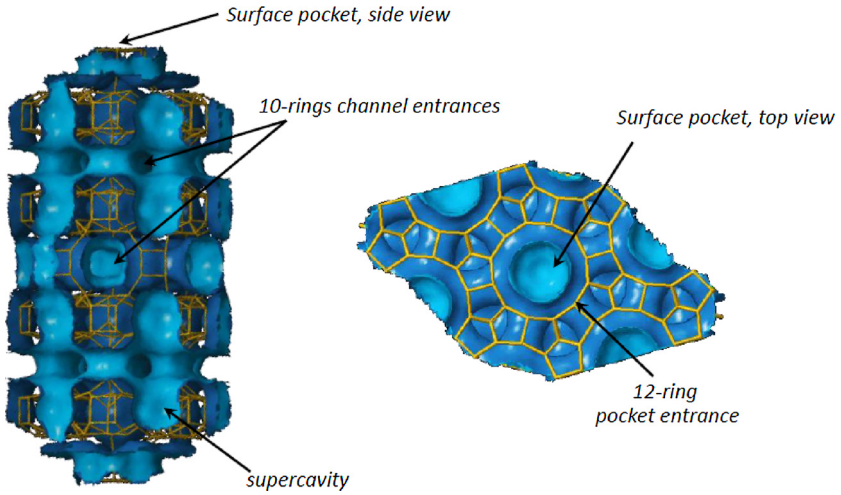

Fig. 1. Channel systems in MWW zeolites. Images created using IZA website animated drawing tool.

having acidity comparable to or even higher than the corresponding 3D zeolites [11], can show improved activity and lifetime in processing of bulky molecules [17–19].

The new potential presented by 2D zeolites in comparison to the conventional 3D zeolite structures is best illustrated by the framework MWW with layers containing internal 10-ring medium pore size sinusoidal channels and 12-ring cavities on the surface (see Fig. 1) [20]. The latter are responsible for the unique activity of MWW zeolites in aromatic alkylation in the form of superior mono-selectivity [21], shown in ethylbenzene and cumene syntheses carried out as large scale industrial processes [22]. The MWW layers are a model to be followed by other 2D zeolites and so far afforded approximately 15 different layered structures directly or by post-synthesis modifications [23]. In particular, they have been found to produce by direct synthesis 7 distinct materials with different layered structures in terms of spatial geometry and connectivity, including the complete 3D connected species (MCM-49). These various materials are formed upon changing synthesis conditions and templates [24]. Details concerning preparation, structure assignment and characterization can be found in prior reports [25,26]. One of these materials, designated MCM-56, is of particular interest as it consists of 2.5 nm thick MWW mono-layers, stacked randomly with little interlayer connectivity [27]. As an apparent delaminated zeolite obtained by direct synthesis MCM-56 is unique [27], without a match by any other zeolite and has demonstrated increased catalytic activity in comparison to the standard MWW zeolites [28]. MCM-56 is also a transient product and is gradually converting to the fully connected 3D framework as the synthesis progresses. Consequently, optimal MCM-56 product is somewhat elusive and needs to be approached by trial-and-error with regard to time of synthesis and formulation. There are now syntheses, e.g. with addition of aniline [29], where MCM-56 is the final product but their downside lies in much extended crystallization time. MCM-56 contains high concentration of Brønsted acid sites (BAS) having Si/Al ratio close to 10, with strong acid centers located not only inside the micropores (a case of majority of zeolites) but also at the external surfaces, in the external cavities (see Fig. 1). Acid centers located inside micropores are available only through 10-rings openings (ca. 5 Å in diameter) imposing diffusion limitation and restraining the access of bulky reactants. The external cups have larger diameters of ca 0.71 nm defined by 12-rings, thus BAS located there may catalyze reactions with less size restrictions. As can be expected, both the degree of layers disorder and the concentration of acid centers in MCM-56 strongly depend on the synthesis procedure because of the mentioned intermediate nature and possible under- or over-crystallization as well as other factors like synthesis mixture composition. The acid characteristics of MCM-56 reported in the literature, e.g. values of acid site concentrations, show significant discrepancies and are often much lower than expected from nominal Si/Al ratio in the synthesis gel [30]. As a transient product MCM-56, which has to be quenched during synthesis at the right but hard to pinpoint moment, is sensitive to various synthesis-related factors, some of which are examined in this work.

As mentioned above, lamellar zeolites combine high acidity of conventional zeolites, easy transport in the interparticle region and facilitated access to the acid centers located inside thin crystals. The test reaction chosen to evaluate these features is the Friedel-Crafts alkylation of mesitylene with benzyl alcohol (Fig. 2). Mesitylene (kinetic diameter 8.60 Å) [31] cannot pass through 10-rings openings of the MWW channels and can react only on the surface. Hence, while two

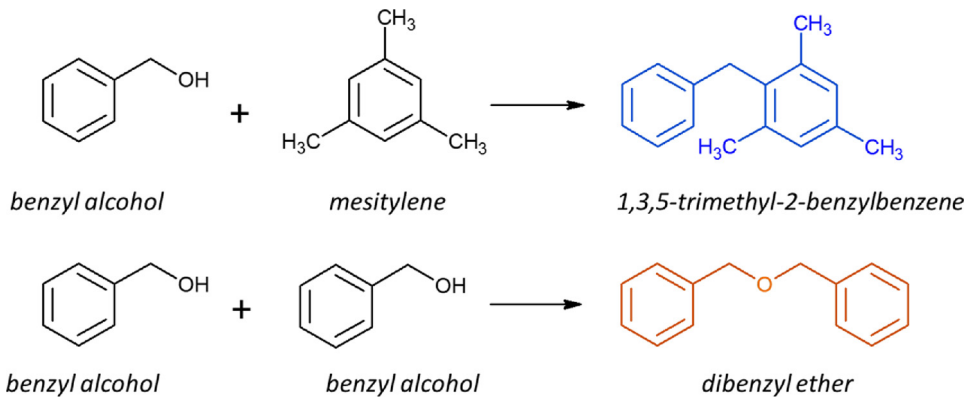

Fig. 2. Friedel-Crafts alkylation of mesitylene with benzyl alcohol.

reactions, alkylation and alcohol etherification, can occur, the former reflects reactivity of the external surfaces. Conversion of the benzyl alcohol depends on the concentration of acid sites, while selectivity to the alkylation or etherification product on the ratio between the sizes of the reactant molecules and zeolite channel diameters [32]. Selectivity to the alkylation product increase with the contact time due to the side reaction converting dibenzyl ether to 1,3,5-trimethyl-2-benzylbenzene [33]. Liu [14], who has been investigating this problem for pillared MWW and ZSM-5 zeolites, quantified Brønsted acid sites localized at the external crystal surfaces and pore-mouth by a combined dimethyl ether titration and methanol dehydration in the presence of selective BAS poisons: 2,6-di-tert-butylpyridine and triphenylphosphine.

In this work we examined MCM-56 zeolites synthesized using different silica sources: Aerosil A200 (fumed silica, Evonic, 200 m^2/g), Ultrasil VN3 (precipitated silica, Grolman, 180 m^2/g) and Ludox (colloidal silica, Sigma Aldrich, LS-30), with hexamethyleneimine as the structure directing agent. Additional synthesis with aniline as structure promoting agent, preventing MCM-56 recrystallization to MCM-49, was also carried out. The obtained MCM-56 samples differed in textural properties, layers organization and the acid properties. They were tested in Friedel-Crafts alkylation of mesitylene with benzyl alcohol to show which property of MCM-56 zeolite is the most essential to obtain the best activity in catalytic reaction of bulky molecules.

2. Experimental

Zeolite syntheses were carried out according to the procedure described in [30] using sodium aluminate (Riedel-de Haen), 50% NaOH (Sigma Aldrich), hexamethyleneimine (HMI, Sigma Aldrich, 99%) and various silicon sources, including Ultrasil (VN3, Grolman), Aerosil (A200, Evonic) and Ludox (LS30, Sigma Aldrich, 30 wt%) in the following molar ratios: Si/Al = 11.5 OH/Si = 0.15, HMI/Si = 0.35 and H_2O/Si = 19.3. Gel mixtures were crystallized for a selected period of time in Teflon lined autoclaves at 143 °C. The obtained products were filtered, washed with deionized water and dried at room temperature overnight. All samples were calcined and ion-exchanged. For calcination, 1 g of a zeolite sample was heated at 540 °C for 6 h (ramp 2 °C/min). The samples were then exchanged using 1 M NH_4NO_3 (≥98%, Sigma Aldrich) three times for 1 h then filtered, washed with deionized water and allowed to dry at room temperature in air.

MCM-56 zeolite with aniline (AN) was synthesized according to the procedure described in the literature [29] using Aerosil A200 as a silicon source, sodium aluminate, 50% NaOH, hexamethyleneimine and aniline (AN, > 99%, Sigma Aldrich) in the following molar ratios: Si/Al = 11.5, OH/Si = 0.18, HMI/Si = 0.1, H_2O/Si = 45 and AN/Si = 0.2. The crystallization was carried out for 176 h and 215 h in a 200 ml Teflon-lined autoclave at 143 °C. The products were activated as above. The names of the samples corresponding to the relevant synthesis procedures are summarized in Table 1.

Nitrogen adsorption isotherms were determined by the standard method at liquid nitrogen temperature using an ASAP 2020 (Micromeritics) static volumetric apparatus. Before adsorption the samples were outgassed at 350 °C using turbomolecular pump.

IR spectra were measured using Tensor 27 from Bruker equipped with MTC detector, at spectral resolution 2 cm^{-1}. Zeolites were pressed into self-supporting wafers with the density of ca 8 mg/cm^2 and activated in situ at 475 °C for 1 h at high vacuum (10^{-5} mBar) in a home-made quartz cell, equipped with KBr windows. Cell construction allowed in situ activation, measurement of the spectra at chosen temperature and adsorption of gases and vapours inside the infrared spectrometer. Before adsorption of a probe molecule the sample was cooled to the proper adsorption temperature: 170 °C for pyridine, and ambient temperature for pivalonitrile. After adsorption of the vapors (ca. 20 mBar equilibrium pressure for both probes) the gas phase together with weakly adsorbed species were desorbed at adsorption temperature for 20 min (pyridine) or 10 min (pivalonitrile). All spectra presented in this paper are recalculated to the same mass of the pellet (10 mg, the pellet surface 3.14 cm^2).

Table 1
Names of the samples corresponding to the relevant synthesis procedures.

Name	silica source	crystallization		structure promoting agent
		time, h	temperature, °C	
A48	Aerosil	48	143	–
A66	Aerosil	66	143	–
A83	Aerosil	83	143	–
A120	Aerosil	120	143	–
A175AN	Aerosil	175	143	aniline
A215AN	Aerosil	215	143	aniline
U40	Ultrasil	40	143	–
U50	Ultrasil	50	143	–
U60	Ultrasil	60	143	–
U70	Ultrasil	70	143	–
L50	Ludox	50	143	–
L54	Ludox	54	143	–
L58	Ludox	58	143	–
L102	Ludox	70	143	–

The concentration of all Lewis (LAS) and Brønsted acid sites (BAS) were evaluated on the basis of pyridine adsorption, using the following absorption coefficients: ε(LAS) = 0.165 cm^2/μmol, and ε(BAS) = 0.044 cm^2/μmol while concentration of external Brønsted acid sites were evaluated on the basis of trimethylacetonitrile (pivalonitrile) adsorption, using absorption coefficient $\varepsilon(BAS_{ext})$ = 0.05 cm^2/μmol [15,30].

For catalytic studies, 50 mg of zeolite sample in the hydrogen form (calcined in air at 500 °C for 5 h, ramp 10 °C/min) was placed in a round bottom flask (50 ml) and then 0.1 g of dodecane (chromatographic internal standard) was added. The flask was put into a parallel synthesis StarFish system under reflux condenser and the mixture was homogenized at reaction temperature (80 °C) for 30 min. Then, 0.2 g of mesitylene was added and this moment was considered as the beginning of the catalytic reaction. Samples were collected at 3, 5, 10, 15, 20, 25, 30, 60, 120, 180, 240, and 300 min. The reaction products were analyzed using gas chromatograph Perkin-Elmer Agilent 7820A, with a FD detector, equipped with a 30 m column DB-5.

3. Results and discussion

Zeolites with MWW topology were crystallized for different times, varying from 40 to 120 h, allowing for monitoring of MCM-56 formation and subsequent conversion into MCM-49. The isolated solid products were evaluated by X-ray diffraction (XRD), N_2 adsorption and FTIR spectroscopy.

Product quality assessment and differentiation between MCM-56 and MCM-49 by X-ray powder diffraction is based on following the shape of the broad band between 8 and 10° 2θ. At the beginning it is without a dip and then shows emerging and deepening valley (Fig. 3). This evolution indicates increasing ordering of the MWW layers, which is disordered for shorter crystallization times (MCM-56) and then forming condensed 3D structure (MCM-49).

For all applied silicon sources, the product in which MCM-56 dominated, was observed only for the shortest crystallization times, ca. 40 h. The ensuing transition to MCM-49 was the slowest when Aerosil was used.

SEM images registered for preparations with the shortest and the longest synthesis time show differences in the morphology of the samples (Fig. 4). For the zeolites with the shortest synthesis time (the highest share of MCM-56), the resulting aggregates are in the form of small, interconnected flakes, while for longest synthesis times (the highest share of MCM-49) – regular, well-formed, and much larger thin flakes. Interestingly, the differences in the crystal morphology are not reflected in changes in the catalytic activity of these materials (apart from the Ultrasil series).

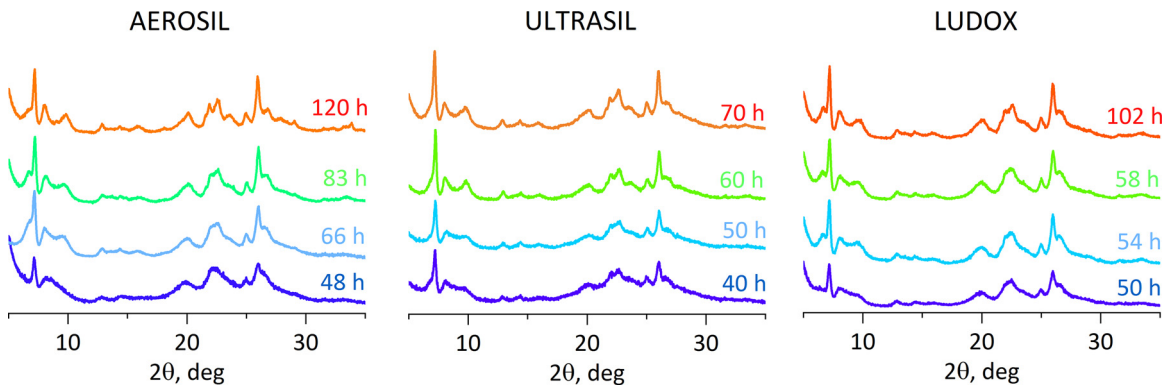

Fig. 3. XRD patterns of as-synthesized MCM-56/MCM-49 samples produced with Aerosil, Ultrasil, and Ludox as silica sources.

Quantitative evaluation of the XRD patterns of MWW zeolites has not been developed sufficiently to allow reliable determination of crystallinity so nitrogen adsorption is used as the supporting tool for assessing product quality (Table 2). Fig. 5 reveals, as a general trend, increasing micropore capacity with increasing crystallization time, which reflects the initial transformation of the amorphous gel into MWW monolayers (MCM-56) and then transformation of the latter into MCM-49 with creation of additional micropores between layers.

The values of the specific surface area are increasing with crystallization time, up to ca. 500 m^2/g, which corresponds to fully crystalline, 3D MCM-49. The observed type of the hysteresis loops (H3 type) closing at $p/p^0 = 0.45$ is characteristic for aggregates of platy particles (Fig. 5) [34]. Crystallization of MCM-56 from the amorphous gel and the 2D (MCM-56) to 3D (MCM-49) conversion overlap, and it is impossible to separate these processes based on nitrogen adsorption alone. The included plot of BET vs. BAS concentration shows that these two parameters are related and increased porosity favors higher acid site concentration. The corresponding trend is parabolic towards 450 m^2/g upper limit and somewhat over 1000 μmol/g BAS, i.e. approaching the value calculated based on Si/Al ratio.

IR spectroscopy was used to monitor MCM-56 formation investigating based on a double band in the range 500–600 cm^{-1}, which corresponds to skeletal vibrations of D6R units of the MWW framework (Fig. 6, Table 2). The integral intensity of this band can be used to quantify zeolite content in a sample [30]. Another maximum, at 800 cm^{-1}, characteristic for stretching symmetric T—O vibrations inside tetrahedra is serving as a measure of all material (crystalline and amorphous) present in the sample, and was used as the normalization factor.

For comparison of various samples of the same zeolite the crucial

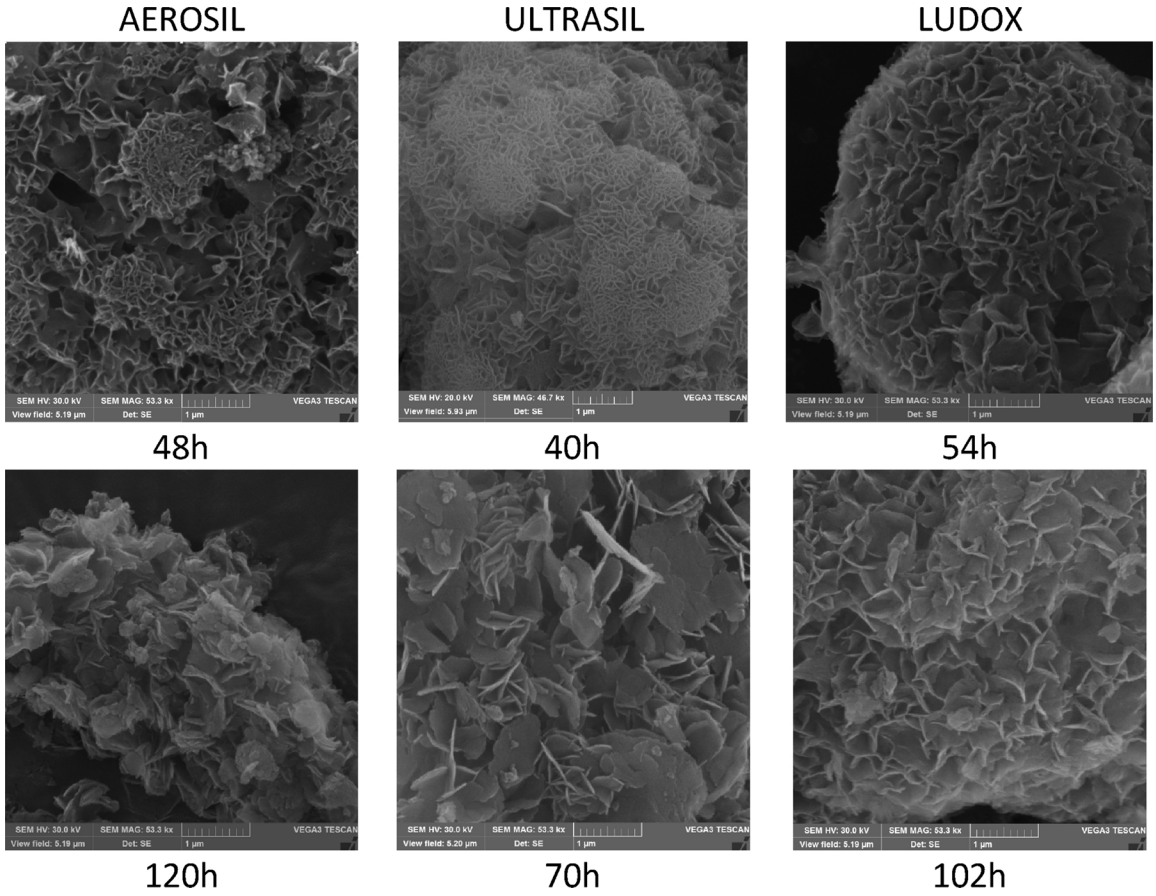

Fig. 4. Comparison of the morphology of the MCM-56/49 preparation from different silica sources at similar stage of development.

Table 2
Textural properties of the studied MCM-56/49 zeolites preparations. BAS and LAS concentrations were calculated using pyridine, BAS_{ext} using trimethylacetonitrile (pivalonitrile) as probe molecules for FTIR studies. Integral intensities (in arbitrary units) of D6R IR maxima were calculated in the range 530-650 cm^{-1}.

Zeolite	BAS, μmol/g	BAS_{ext}, μmol/g	LAS, μmol/g	S_{BET}, m^2/g	S_{ext}, m^2/g	v_{micro}, cm^3/g	D6R intensity
A48	535	274	129	328	158	0.030	1.12
A66	607	420	173	445	159	0.087	1.23
A83	892	380	74	434	112	0.105	1.33
A120	942	364	156	463	107	0.112	2.01
A175AN	913	269	91	436	146	0.089	1.48
A215AN	856	257	97	456	111	0.115	1.45
U40	353	59	25	123	31	0.026	0.38
U50	432	139	61	250	47	0.060	0.86
U60	674	139	70	382	138	0.063	1.66
U70	844	262	112	453	37	0.140	2.01
L50	721	282	110	311	64	0.066	1.48
L54	771	382	120	431	128	0.103	1.86
L58	885	428	97	402	72	0.096	1.92
L102	1042	356	126	422	76	0.110	2.07

parameter is the acidity, understood as comprising the type, concentration and accessibility of the acid centers. Acidity may be evaluated by FTIR spectroscopy applying proper probe molecules [13,35]. In this work pyridine was chosen as a probe molecule able to access all the acid centers, and trimethylacetonitrile (pivalonitrile) of critical diameter 0.62 nm [36], as the probe able to react only with external acid sites both inside the external surface cups and located at pore mouths.

With increasing zeolite content, quantified as the integral of D6R IR maxima, the concentration of all BAS was increasing, as indicated by the maximum characteristic of Si−OH-Al groups becoming more intense (Fig. 6). At the same time, the amount of extraframework, or partially framework Al species, with characteristic IR maximum at 3660 cm^{-1} remained practically constant. The concentration of LAS also did not change considerably with synthesis time (Table 2).

Some clear trends can be observed (Fig. 7) – BET area, followed by the micropore volume, and total concentration of BAS increase with synthesis time up to certain level, characteristic for fully condensed MCM-49 (ca 450 m^2/g) and limited by the amount of Al in the synthesis gel. The variable that does not follow this trend is concentration of the BAS located at the external surfaces (BAS_{ext}).

For Aerosil series the concentration of BAS_{ext} is almost constant (400–450 μmol/g with tendency to slight decrease), the same trend is observed for BET and total BAS concentration. V_{micro} is increasing, which testifies about continuous condensation of the layers; the first product (obtained after 48 h) has almost pure MCM-56 character and all others are the MCM-56/MCM-49 mixtures. For Ultrasil series the concentration of BAS_{ext} is increasing to ca 220 μmol/g, while at the same time total BAS concentration is almost linearly increasing. This means that increasing synthesis time over 50 h causes thickening of the crystals, the product is already condensed (MCM-49), because no increase in micropore volume is observed. For Ludox the BAS_{ext} concentration increases sharply initially and then suddenly drops (60–100 hours), which could be a mark of layer condensation. The micropore volume is constant above 70 h, suggesting complete framework formation with subsequent changes in other parameters corresponding to crystal coarsening. In conclusion, evaluation of at least two parameters – micropore volume and concentration of external BAS can be used to determine quality of MCM-56 materials.

Since it is assumed that for Friedel-Crafts alkylation of benzyl alcohol with mesitylene the formation of alkylation product should proceed only on the external surfaces, the catalyst that will probably show the best catalytic properties could be proposed. For Aerosil series A66 has the highest concentration of BAS_{ext} (420 μmol/g), for Ultrasil it is U70 (BAS_{ext} 262 μmol/m^2), and for Ludox series L58 (BAS_{ext} 428 μmol/g). In all cases alkylation reaction prevailed over etherification and for all tested zeolites the selectivity (after 30–60 minutes of reaction) was ca. 90% for alkylation product. With prolonged contact time selectivity to 1,3,5-trimethyl-2-benzylbenzene increased due to the side reaction converting dibenzyl ether to the alkylation product (Fig. 8 and Table 3).

To quantify catalytic activity by one parameter, T_{50} denoting the time when 50% conversion of benzyl alcohol was reached, was chosen. This value was calculated from the linear equation fitted to the data for the first 30 min of reaction and the results are presented in Table 3.

Analyzing the data presented in Fig. 8 it can be seen that three samples form the Aerosil series have very similar catalytic activity, with A66 being marginally superior. For the Ultrasil series, U70 with the highest BAS_{ext} concentration showed the best catalytic performance, while for Ludox series L58 and L102 have practically the same activity. Since all reactions were carried out under exactly the same conditions, the catalytic activity of each sample can be directly compared. In all cases the optimal material for each silica source – in terms of external Brønsted acid sites concentrations – showed the best catalytic performance (Fig. 9).

Another parameter that allows a direct comparison of the catalytic activity of different catalytic systems is turnover frequency (TOF). TOF are also a function of the nature of the surface active sites. TOF were calculated for the same conversion of benzyl alcohol (50%). In our case, the values between 0.62 (sample L54) and 1.06 min^{-1} (sample A175AN) were obtained. The TOF values for all cases are of the same order of magnitude, probably the external BAS are also similar in terms of accessibility and acid strength.

Friedel-Crafts alkylation may be also catalyzed on Lewis acid centers and, in the case of the presented here series, the share of LAS reaches in some cases 40% of all acid sites, especially for samples with

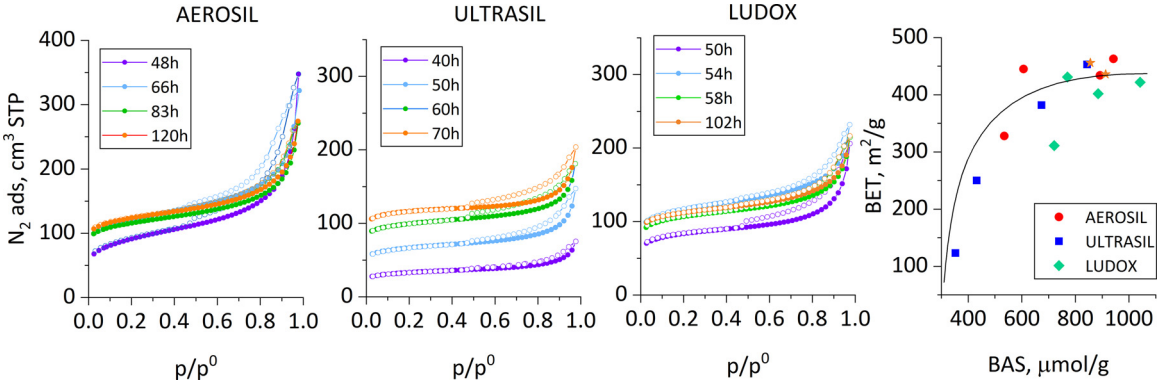

Fig. 5. N_2 adsorption isotherms for MCM-56/MCM-49 samples synthesized with Aerosil, Ultrasil, and Ludox as silica sources. Isotherms are not shifted. Dependence of BET area on BAS concentration is also presented.

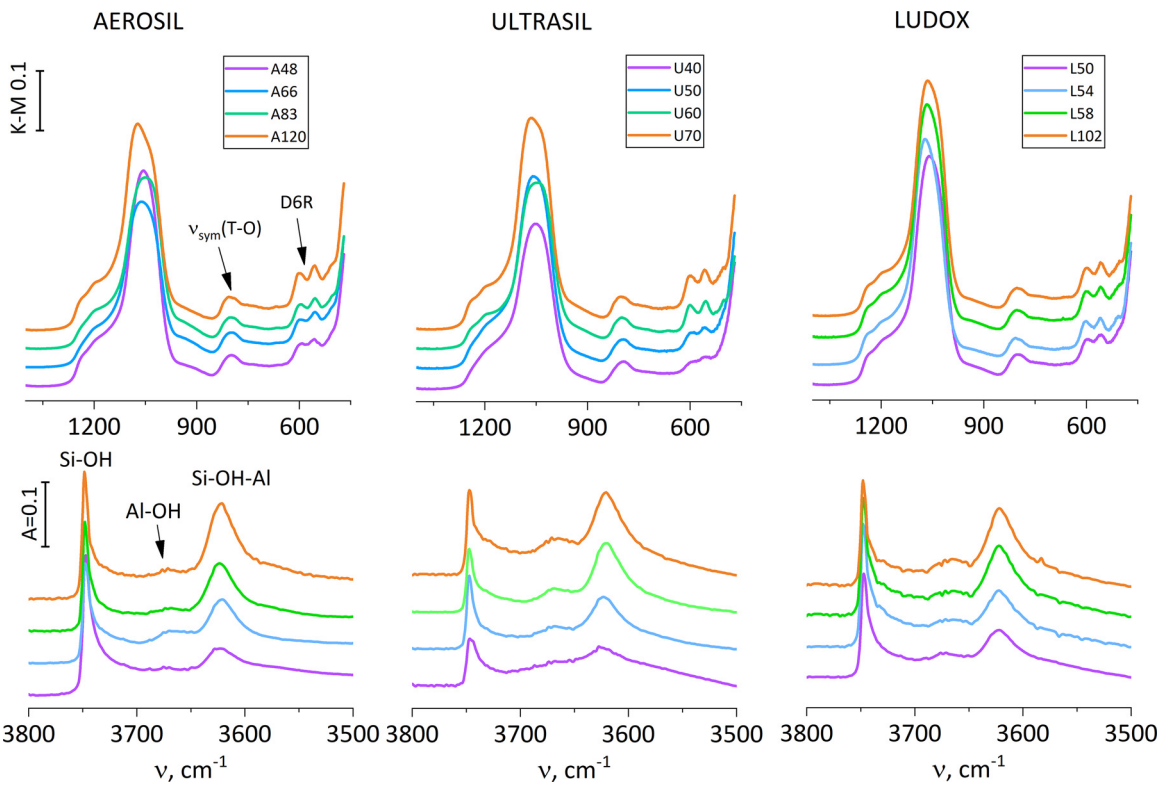

Fig. 6. IR spectra of MCM-56/MCM-49 samples synthesized with Aerosil, Ultrasil, and Ludox as silica sources. Upper panes: IR spectra (ATR mode, Kubelka-Munk scale) in the region of the skeletal vibrations. Spectra normalized to integrated intensity of the 800 cm^{-1} band. Lower panes: IR spectra (absorbance mode) in the region of O—H vibrations. All samples activated at 470 °C, spectra at 170 °C, normalized to a 10 mg sample.

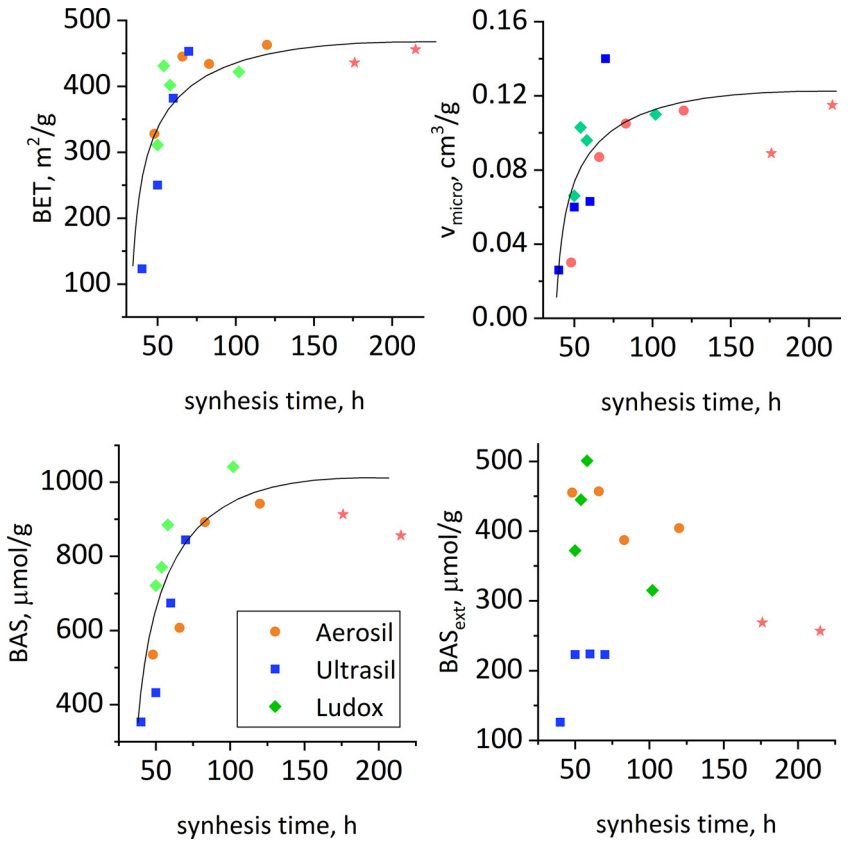

Fig. 7. Dependence of the BET area, micropore volume, total BAS and external BAS concentration on synthesis time for MCM-56/MCM-49 samples combined for all silica sources. MCM-56 samples synthesized with aniline as structure promoting agent are marked with asterisks.

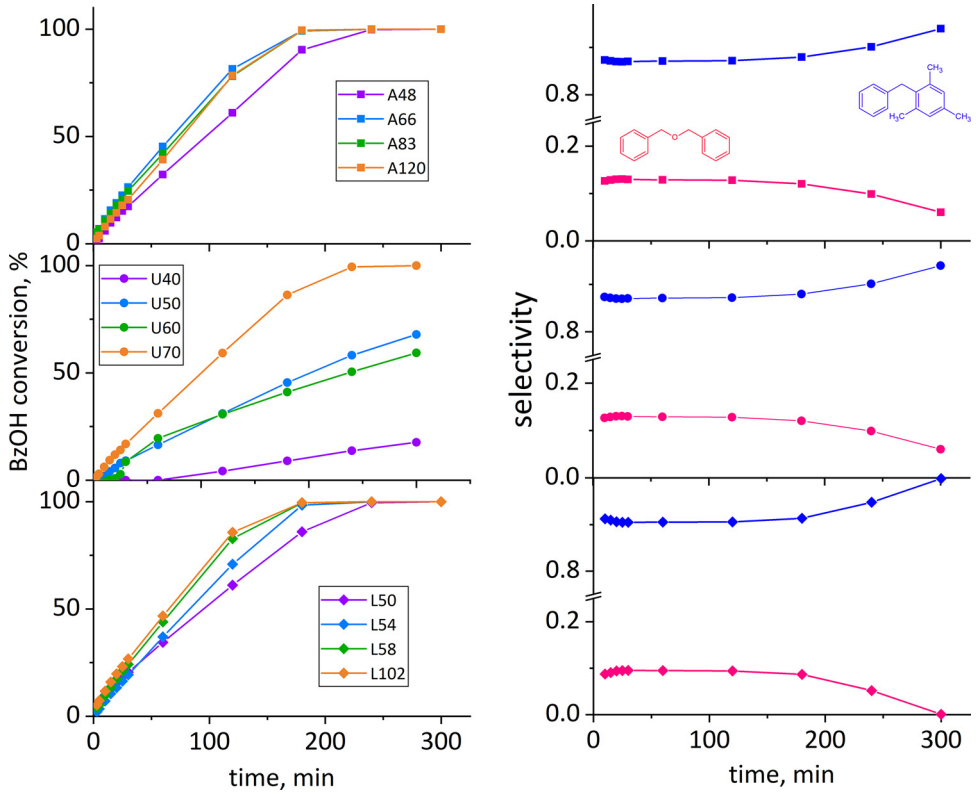

Fig. 8. Catalytic test results. Conversion of benzyl alcohol for all tested materials and selectivity to alkylation and etherification product for the most active materials in each series: A66, U70 and L102.

Table 3
Catalytic test results. T_{50} is the time when 50% conversion of benzyl alcohol was reached. TOF calculated at t_{50}. Benzyl alcohol (BzOH) conversion and selectivities to 1,3,5-trimethyl-2-benzylbenzene (alkylation) and dibenzyl ether (etherification) was measured after 30 min of reaction.

Zeolite	t_{50}	BzOH	TOF	selectivity, %	
	min	conv, %	min^{-1}	etherification	alkylation
A48	80	17.4	0.84	10.5	89.5
A66	64	26.4	0.69	11.6	88.4
A83	71	24.6	0.69	9.1	90.9
A120	74	20.5	0.69	10.8	89.2
A175AN	65	24.9	1.06	11.1	88.9
A215AN	77	19.1	0.93	10.2	89.8
U40	422	0	0.74	13.7	86.3
U50	137	9.1	0.97	12.8	87.2
U60	140	8.6	0.95	11.5	88.5
U70	89	16.9	0.79	12.8	87.2
L50	86	20.6	0.76	10.1	89.9
L54	78	19.4	0.62	10.3	89.3
L58	66	24.2	0.65	9.5	90.5
L102	63	26.7	0.82	9.4	90.6

low concentration of BAS. However, the role of LAS is quite complex. According to well established mechanism [37], LAS may produce carbocation from the alcohol in two-stage reaction for which formation of carbocation (or alcohol-LAS complex) is the rate determining step. Recently, Nur et al. [38] suggested synergistic role of Lewis and Brønsted acid centers in Friedel-Crafts alkylation. They also proposed a mechanism in which BAS are responsible for the formation of carbocation from alcohol, while the LAS interaction with the aromatic ring of hydrocarbons facilitates consecutive alkylation reaction. In our case, no clear-cut trend between concentration of LAS and catalytic activity or selectivity to any of reaction product was found.

Recently, Zhang et al. [39] reported a remarkable observation that

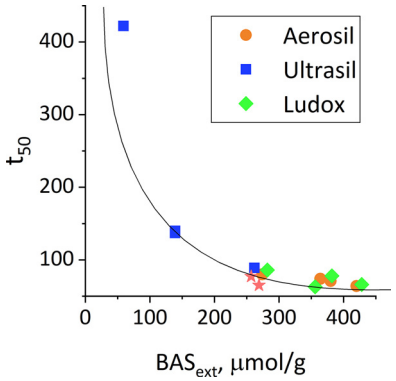

Fig. 9. Catalytic activity dependence on the concentration of external Brønsted acid sites for MCM-56/MCM-49 samples synthesized with Aerosil, Ultrasil, and Ludox as silica sources. T_{50} is the time when 50% conversion of benzyl alcohol was reached. MCM-56 samples synthesized with aniline as structure promoting agent are marked with asterisks.

adding aniline to MCM-56 synthesis mixture prevented layer condensation and conversion of MCM-56 into MCM-49, making the former the end product. Since the acidic properties of the synthesized samples were not characterized we thought it is worthwhile to include their characterization in this work.

Two MCM-56 samples were obtained, synthesized for 176 and 215 h, and confirmed the reported role of aniline addition as effectively stopping conversion to the 3D structure MCM-49. The analysis of diffractograms of the tested materials (Fig. 10) shows that significant prolongation of the synthesis time (above 120 h) does not cause the formation of MCM-49 or even the MCM-56/49 mixture. The XRD profiles of both materials are practically identical and are typical for layered, disorganized MCM-56 zeolite with a characteristic unresolved band at 8-10° 2θ.

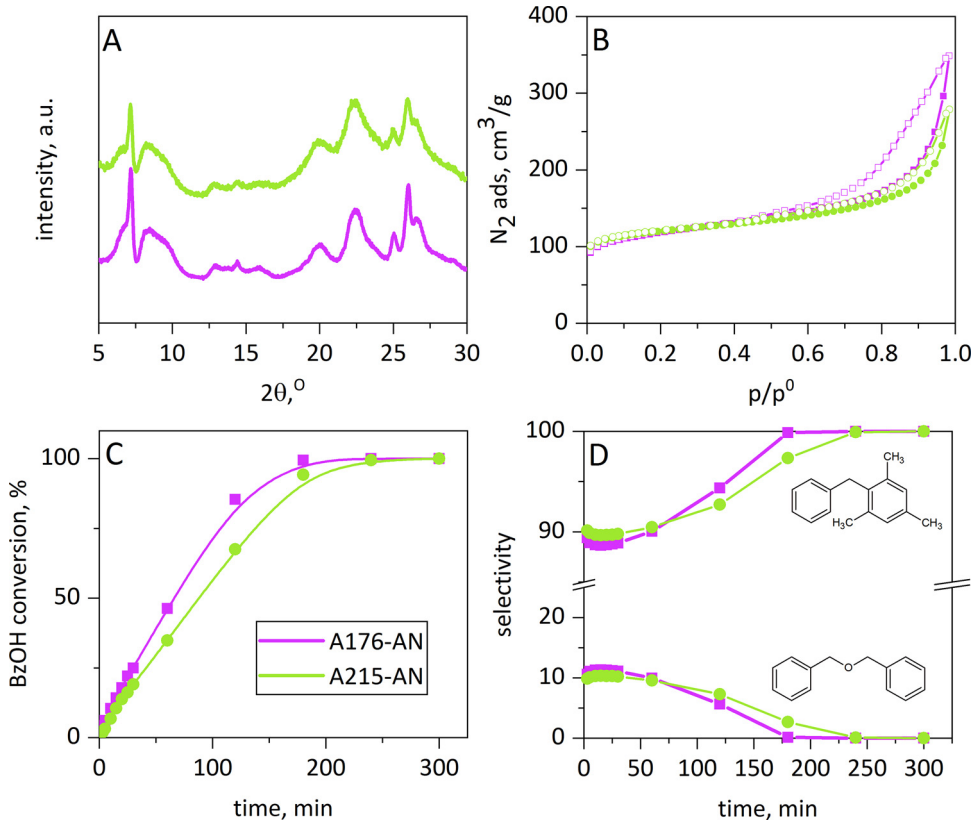

Fig. 10. XRD patterns (A) and nitrogen adsorption isotherms (B) for MCM-56 synthesized with aniline for 176 and 215 h, together with catalytic test results: conversion of benzyl alcohol (C), and selectivity to alkylation and etherification products (D).

Textural parameters determined on the basis of the obtained nitrogen adsorption isotherms indicate that these materials have significantly increased micropores volume, comparable to previously obtained MCM-56/-49 zeolites with the longest synthesis times (about 0.115 cm^3/g), high BET surface area (450 m^2/g) and high share of the external surface, although the latter decreases significantly during the extension of the synthesis time (from 146 to 111 m^2/g). Acidity of the obtained materials also fit the textural parameters and morphology (Table 2). Both samples have very high concentration of BAS (850–900 μmol/g), significantly higher than A48 of the shortest synthesis time and purely MCM-56 character (530 μmol/g) and comparable to A120 (longest synthesis time), of mostly MCM-49 character (940 μmol/g). The share of Lewis-type centers in these preparations was also small, not exceeding 100 μmol/g. It seems that the addition of aniline to delay layers condensation forms specific 'hybrids' that combine the best features of 2D zeolites, such as high external surface and resulting from this enhanced availability of acid centers (BAS_{ext} 250 μmol/g), and the best features of 3D zeolites – increased concentration of acid centers. In line with these features, 'hybrids' show high and similar catalytic properties to MCM-56 zeolites with the highest MCM-49 share. The results for the longest synthesis time (215 h) showing decreased catalytic properties indicates that prolonging the synthesis too much may show activity deterioration maybe as a result of decreasing external BAS.

4. Conclusions

In this work a series of MCM-56 and MCM-49 samples synthesized for different times using Aerosil, Ultrasil and Ludox as silica sources, hexamethyleneimine as the structure directing agent and additionally aniline as structure promoting agent was investigated. Synthesized materials differed in acid properties and degree of layers organization. With longer synthesis time the zeolite content, total Brønsted acid sites concentration, BET area and micropore volume were gradually increasing.

Catalytic activity in the test reaction of Friedel-Crafts alkylation of mesitylene with benzyl alcohol depended on the concentration of the Brønsted acid centers located at the external surfaces of the zeolite crystals.

Addition of aniline to delay layers condensation forms specific 'hybrids' that combine high external surface and enhanced availability of Brønsted acid centers of MCM-56 with increased total concentration of acid centers, characteristic for MCM-49. This also results in high catalytic activity of such materials. Further prolongation of crystallization decreases catalytic activity of the resulting sample.

The key role in correlating physical characteristic with catalytic activity was played by infrared spectroscopy, enabling to study many properties of the tested materials, such as concentration of acid centers, and their type (Brønsted or Lewis acids), concentration of centers available for the reagent molecules, to investigating the correlation of acidity with the degree of zeolite crystallinity.

Acknowledgement

This work was financed with the funds from the National Science Centre Poland, grant no 2016/21/B/ST5/00858, MK acknowledges Czech Science Foundation (Project ExPro 19-27551X).

References

[1] A. Primo, H. Garcia, Zeolites as catalysts in oil refining, Chem. Soc. Rev. 43 (2014) 7548–7561.
[2] W. Vermeiren, J.P. Gilson, Impact of zeolites on the petroleum and petrochemical industry, Top. Catal. 52 (2009) 1131–1161.
[3] T.F. Degnan, Recent progress in the development of zeolitic catalysts for the petroleum refining and petrochemical manufacturing industries, From Zeolites to Porous MOF Materials: the 40th Anniversary of International Zeolite Conference,

Proceedings of the 15th International Zeolite Conference, (2007), pp. 54–65 170.
[4] R.A. Sheldon, R.S. Downing, Heterogeneous catalytic transformations for environmentally friendly production, Appl. Catal. A-Gen. 189 (1999) 163–183.
[5] M.G. Clerici, Zeolites for fine chemicals production, Top. Catal. 13 (2000) 373–386.
[6] J. Přech, P. Pizarro, D.P. Serrano, J. Čejka, From 3D to 2D zeolite catalytic materials, Chem. Soc. Rev. 47 (2018) 8263–8306.
[7] M. Danilczuk, K. Dlugopolska, T. Ruman, D. Pogocki, Molecular sieves in medicine, Mini-Rev. Med. Chem. 8 (2008) 1407–1417.
[8] M.I. Carretero, M. Pozo, Clay and non-clay minerals in the pharmaceutical industry Part I. Excipients and medical applications, Appl. Clay Sci. 46 (2009) 73–80.
[9] A.C. Lopes, P. Martins, S. Lanceros-Mendez, Aluminosilicate and aluminosilicate based polymer composites: present status, applications and future trends, Prog. Surf. Sci. 89 (2014) 239–277.
[10] A. Bruckner, Looking on heterogeneous catalytic systems from different perspectives: multitechnique approaches as a new challenge for in situ studies, Catal. Rev. Sci. Eng. 45 (2003) 97–150.
[11] J.A. Boscoboinik, X. Yu, E. Emmez, B. Yang, S. Shaikhutdinov, F.D. Fischer, J. Sauer, H.J. Freund, Interaction of probe molecules with bridging hydroxyls of two-dimensional zeolites: a surface science approach, J. Phys. Chem. C 117 (2013) 13547–13556.
[12] P.B. Venuto, Structure-reactivity-selectivity relationships in reaction of organics over zeolite catalysts, in: H. Chon, S.K. Ihm, Y.S. Uh (Eds.), Studies in Surface Science and Catalysis, Elsevier, 1997, pp. 811–852.
[13] J.C. Lavalley, Infrared spectrometric studies of the surface basicity of metal oxides and zeolites using adsorbed probe molecules, Catal. Today 27 (1996) 377–401.
[14] Y. Wu, L. Emdadi, D. Qin, J. Zhang, D. Liu, Quantification of external surface and pore mouth acid sites in unit-cell thick pillared MFI and pillared MWW zeolites, Microporous Mesoporous Mater. 241 (2017) 43–51.
[15] B. Gil, K. Kałahurska, A. Kowalczyk, A study of the external and internal sites of 2D and 3D zeolites through the FTIR investigation of the adsorption of ammonia and pivalonitrile, Appl. Catal. A Gen. 578 (2019) 63–69.
[16] K. Moller, T. Bein, Mesoporosity - a new dimension for zeolites, Chem. Soc. Rev. 42 (2013) 3689–3707.
[17] D. Liu, X. Zhang, A. Bhan, M. Tsapatsis, Activity and selectivity differences of external Brønsted acid sites of single-unit-cell thick and conventional MFI and MWW zeolites, Microporous Mesoporous Mater. 200 (2014) 287–290.
[18] J.-C. Kim, K. Cho, R. Ryoo, High catalytic performance of surfactant-directed nanocrystalline zeolites for liquid-phase Friedel–Crafts alkylation of benzene due to external surfaces, Appl. Catal. A Gen. 470 (2014) 420–426.
[19] M. Choi, K. Na, J. Kim, Y. Sakamoto, O. Terasaki, R. Ryoo, Stable single-unit-cell nanosheets of zeolite MFI as active and long-lived catalysts, Nature 461 (2009) 246-U120.
[20] M.E. Leonowicz, J.A. Lawton, S.L. Lawton, M.K. Rubin, MCM-22 - a molecular-sieve with 2 independent multidimensional channel systems, Science 264 (1994) 1910–1913.
[21] J.C. Cheng, T.F. Degnan, J.S. Beck, Y.Y. Huang, M. Kalyanaraman, J.A. Kowalski, C.A. Loehr, D.N. Mazzone, A comparison of zeolites MCM-22, beta, and USY for liquid phase alkylation of benzene with ethylene, in: H. Hattori, K. Otsuka (Eds.), Studies in Surface Science and Catalysis, Elsevier, 1999, pp. 53–60.
[22] T.F. Degnan Jr., C.M. Smith, C.R. Venkat, Alkylation of aromatics with ethylene and propylene: recent development in commercial processes, Appl. Catal. A Gen. 221 (2001) 283–294.
[23] W.J. Roth, B. Gil, W. Makowski, B. Marszalek, P. Eliasova, Layer like porous materials with hierarchical structure, Chem. Soc. Rev. 45 (2016) 3400–3438.
[24] J. Grzybek, W.J. Roth, B. Gil, A. Korzeniowska, M. Mazur, J. Čejka, R.E. Morris, A new layered MWW zeolite synthesized with the bifunctional surfactant template and the updated classification of layered zeolite forms obtained by direct synthesis, J. Mater. Chem. A 7 (2019) 7701–7709.
[25] W.J. Roth, J. Cejka, R. Millini, E. Montanari, B. Gil, M. Kubu, Swelling and interlayer chemistry of layered MWW zeolites MCM-22 and MCM-56 with high Al content, Chem. Mater. 27 (2015) 4620–4629.
[26] W.J. Roth, D.L. Dorset, Expanded view of zeolite structures and their variability based on layered nature of 3-D frameworks, Microporous Mesoporous Mater. 142 (2011) 32–36.
[27] W.J. Roth, MCM-22 zeolite family and the delaminated zeolite MCM-56 obtained in one-step synthesis, Stud. Surf. Sci. Catal. 158A and B (2005) 19–26.
[28] J.C. Cheng, A.D. Fung, D.J. Klocke, S.L. Lawton, D.N. Lissy, W.J. Roth, C.M. Smith, D.E. Walsh, Process for preparing short chain alkyl aromatic compounds, U.S. Patent, Mobil Oil Corp., USA, 1995.
[29] E. Xing, Y. Shi, W. Xie, F. Zhang, X. Mu, X. Shu, Perspectives on the multi-functions of aniline: cases from the temperature-controlled phase transfer hydrothermal synthesis of MWW zeolites, Microporous Mesoporous Mater. 254 (2017) 201–210.
[30] B. Gil, W.J. Roth, W. Makowski, B. Marszalek, D. Majda, Z. Olejniczak, P. Michorczyk, Facile evaluation of the crystallization and quality of the transient layered zeolite MCM-56 by infrared spectroscopy, Catal. Today 243 (2015) 39–45.
[31] S.F. Zaman, K.F. Loughlin, S.A. Al-Khattaf, Kinetics of desorption of 1,3-Diisopropylbenzene and 1,3,5-Triisopropylbenzene. 2. Diffusion in FCC catalyst particles by zero length column method, Ind. Eng. Chem. Res. 54 (2015) 4572–4580.
[32] J. Čejka, B. Wichterlová, Acid-catalyzed synthesis of mono- and dialkyl benzenes over zeolites: active sites, zeolite topology, and reaction mechanisms, Catal. Rev. 44 (2002) 375–421.
[33] N. Narender, K.V.V.K. Mohan, S.J. Kulkarni, I.A.K. Reddy, Liquid phase benzylation of benzene and toluene with benzyl alcohol over modified zeolites, Catal. Commun. 7 (2006) 583–588.
[34] K.S.W. Sing, R.T. Williams, Physisorption hysteresis loops and the characterization of nanoporous materials, Adsorpt. Sci. Technol. 22 (2004) 773–782.
[35] G. Busca, Acidity and basicity of zeolites: a fundamental approach, Microporous Mesoporous Mater. 254 (2017) 3–16.
[36] T. Armaroli, M. Trombetta, A.G. Alejandre, J.R. Solis, G. Busca, FTIR study of the interaction of some branched aliphatic molecules with the external and internal sites of H-ZSM5 zeolite, J. Chem. Soc. Faraday Trans. 2 (2000) 3341–3348.
[37] R.T. Morrison, Organic chemistry/Robert Thornton Morrison, Robert Neilson Boyd, Allyn and Bacon, Boston, 1973.
[38] H. Nur, Z. Ramli, J. Efendi, A.N.A. Rahman, S. Chandren, L.S. Yuan, Synergistic role of Lewis and Brönsted acidities in Friedel–Crafts alkylation of resorcinol over gallium-zeolite beta, Catal. Commun. 12 (2011) 822–825.
[39] E.H. Xing, Y.C. Shi, W.H. Xie, F.M. Zhang, X.H. Mu, X.T. Shu, Temperature-controlled phase-transfer hydrothermal synthesis of MWW zeolites and their alkylation performances, RSC Adv. 6 (2016) 29707–29717.